GULLY SLOPES AND DISCHARGES ON LYOT CRATER'S CENTRAL PEAK. S. D. Hart[1], V. C. Gulick[1], R.A. Parsons[2] and C.J. Barnhart[2], [1]NASA Ames Research Center, M/S 239-20, Moffett Field, CA 94035-1000 (shawn.d.hart@nasa.gov), [2]U.C. Santa Cruz, Earth & Planetary Sciences Department, Earth & Marine Sci., Santa Cruz, CA 95064.

Introduction: Since the discovery of gullies on some crater slopes and valley walls [1], there have been several hypotheses put forth concerning their origin and formation [2-10]. This study focuses on gullies that are located on the central peak of Lyot crater located in the Northern Plains of Mars (50.4N, 29.3E). The gullies source between 150m and 750m below the top of the central peak. A previous study by Dickson and Head [11] of gullies on topographic highs used MOC images and MOLA profiles to observe several areas where gullies are present, concluding that they were the result of the melting of a snow pack that had been deposited on the topographic high. Here we study well defined gullies present on the central peak of the impact crater Lyot, an Amazonian-aged, multi-ring impact basin that is 215km in diameter. We use a high-resolution set of stereo images provided by the HiRISE camera on the Mars Reconnaissance Orbiter (MRO) to perform a thorough analysis of meter-scale gully features and present a high resolution set of slope profiles. We then use this detailed elevation data to determine discharge estimates for the two major gullies on Lyot's central peak using methods formulated by Ikeda [12] and Kleinhans [13].

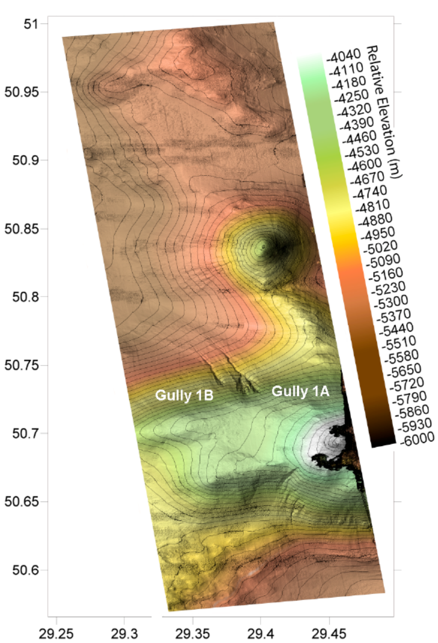

Figure 1. DEM produced by Socet Set using HiRISE stereo images of Lyot's central peak. The two main gullies are apparent in the lower middle portion and tend Northward. Credit Charles Barnhart.

Methods: During this study we've focused on creating accurate slope measurements along gully profiles, and calculating discharge estimations based on these and channel geometry.

Gully Profiles.

We used three methods for profile creation: 1) The first was developed by Kreslavsky [14], in which spacecraft viewing geometry and an observed parallax between two points in the two stereo images is used to calculate a change in elevation. We identify small objects or features common to both images to accurately determine position within the image at the pixel scale (these points are selected by hand using GIS software). Next, the relative shift in position between the pair of points in the two images gives a parallax vector. The parallax vector orientation is ideally determined by the two camera viewing orientations and its length is proportional to the difference in elevation between the objects. Observed parallax vector orientation deviate slightly from the predicted orientation allowing us to determine the error. Typical errors in slope using this method are between 0.5 to 2 degrees over 100m length scales. 2) Profiles are also generated using MOLA data. Using the commercial program Surfer(R), we constructed a Digital Elevation Model (DEM) from MOLA (Mars Orbiter Laser Altimeter) PEDR (Precision Experiment Data Records) data. Using this DEM we followed the trace of the gullies, creating an elevation profile. 3) The third method involved creating a complete DEM from the HiRISE stereo pair using the Socet-Set software package, and importing this into ENVI for profile measurements along the gullies. This method created a DEM with a vertical resolution of roughly 4m.

Discharge Estimates.

We estimate bank-full fluvial discharge and flow velocity in the two prominent gullies 1A and 1B (see Figure 1). Though we have employed empirical terrestrial formulas for calculating flow rates such as the Manning equation [15-17], the lack of gravity scaling has led us to base our discharge estimates on work in which differences in slope, gravity, and grainsize can be quantified. Discharge in m^3/s is given by

$$Q = uWh \qquad (1)$$

where u is mean flow velocity, W is channel width, and h is the depth of the channel. We assume a 1:8 depth to width ratio to determine channel depth [18], and implement theory from Kleinhans [13] and Ikeda [12] with observed channel geometry, channel sinuosity, and slope measurements to calculate a discharge.

The width-averaged flow velocity based on [13] is given by

$$u_K = (8ghS/f)^{1/2} \quad (2)$$

where g is gravity, S is the local slope (in radians), and f is an empirical friction factor that depends on the bed roughness and the local slope as shown in this equation [13]:

$$f = (8/4.84)(a^{0.055}S^{0.275})^2 \quad (3)$$

where a is equal to h divided by the median grainsize D50 (smaller grainsizes tend to give smaller discharge estimates). The critical assumption in this calculation is the median grainsize, which cannot currently be resolved at the scale of gully channels from remote sensing. We calculate flow velocity using two different median grainsizes: 0.3mm and 1cm.

An alternative method of calculating flow velocity takes advantage of the wavenumber of channel meandering (k). Using this additional observation to constrain the flow velocity, frees us from making an assumption about median grainsize. k can be related to channel flow velocity using an equation from [12]:

$$k = 2\pi/\lambda = \frac{2C_f((0.5(A + 2 + F^2))^{1/2} - 1)^{1/2}}{h} \quad (4)$$

where λ is the meander wavelength and A is an empirical constant equal to 2.89 for alluvial streams. The Froude number (F) and the friction factor (C_f) are given by

$$F = u_I/(gh)^{1/2} \quad (5)$$

$$C_f = ghS/u_I^2 \quad (6)$$

respectively, where u_I is the flow velocity. Because equation 4 cannot be analytically solved for u_I using equations 5 and 6, we must choose an initial value and then iteratively solve for the flow velocity (u_I) in equation 4 using the given values for h, S , g, and λ .

Discharge Estimates		
	Gully 1A	**Gully 1B**
Channel Width (m)	6.25 5.5 8.5 11 – 22	7.5 – 30.5 5.75 2.1 – 15.5
Channel Height (m) (1/8 = depth/width)	0.8 0.7 1.1 1.4 – 2.7	0.9 – 3.8 0.7 0.3 – 1.9
Slope (degrees)	9.5	10.5
Q Kleinhans (m^3/s)	9 6.5 19.4 6.8	13 0.7 83
Kleinhans Velocity (m/s)	1.8 1.7 2.1 2.7	2 1.1 2.8
Meander Wavelength (m)	60-120	80
Q Ikeda (m^3/s)	17.8-49.8	30.4 3.1 130
Ikeda Velocity (m/s)	3.5-5.3	4.5 4.4 4.9

Table 1. Represents measurements and results for the two largest gullies present on Lyot Crater's central peak.

Summary: We present our observations of gully features on the central peak of Lyot crater, including detailed analysis of geomorphic features, high-resolution profile data, and estimations of fluid discharge. High resolution HiRISE images with a ground scale between 31.7cm/pixel and 30.9cm/pixel were used to analyze meter-scale features within the gullies. Features such as eroded bedrock, sinuous channels, incised escarpments, point bars, anastamosing channels, superposition of channels, and deposition of apparent fine sediment on the debris aprons were observed in the two most highly developed gullies. High-resolution profiles were made of the two most prominent gullies present on the central peak. Slopes were then calculated, which range from 16.4° to 29.7° for the alcoves, 11.3° to 20.6° for the channels, and 8.4° to 16.9° for the debris aprons. Discharge estimates using [13], a grainsize of 0.3mm and 10 mm, and bank-full flow discharge in gullies 1A and 1B range from 0.75 to 83 m^3/s and 8.6 to 22 m^3/s, respectively. The discharge estimates using [12] method range from 8.0 to 83 m^3/s for gully 1A, and from 21 to 47 m^3/s for gully 1B. The origin of these gullies is still unknown, but these detailed observations, discharge calculations, and the unique location of these gullies should help to constrain future origin hypotheses.

References:

[1] Malin M.C. and Edgett K.S. (2000) *Science, 288,* 2330. [2] Musselwhite D.S. et al. (2001) *GRL, 28(7),* 1283-1285. [3] Mellon M.T. and Phillips R.J. (2001) *JGR, 106(0),* 1-15. [4] Gaidos E.J. (2001) *Icarus, 153,* 218-223. [5] Gilmore M.S. and Goldenson N. (2004) *LPS XXXV,* 1884. [6] Costard F. et al. (2002) *Science, 295,* 110. [7] Lee P. et al. (2002) *LPS XXXIII,* 2050. [8] Hartmann W.K. et al. (2003) *Icarus, 162,* 259-277. [9] Christensen P.R. (2003) *Nature, 422,* 45-48. [10] Treiman A.H. (2003) *JGR, 108,* E4. [11] Dickson J.L. et al. (2007) *Icarus, 188,* 315-323. [12] Ikeda S. et al. (1981) *J. Fluid Mech., 112,* 363-377. [13] Kleinhans M.G. (2005) *JGR, 110,* E12003. [14] Kreslavsky (2008) *LPS XXXIX,* 2328. [15] Burr D. (2002) *GRL, 29(1),* 1013. [16] Kereszturi A. (2003) *Sixth Conf. Mars,* 3039. [17] Wilson L. et al. (2004) *JGR, 109,* E09003. [18] Howard A.D. et al. (2008) *LPS XXXIX,* 1629.

Additional Information: If you have any questions or need additional information you may contact Shawn Hart at Shawn.D.Hart@nasa.gov.